

3D-Modeling of Ingot Geometry Development of DC-Cast Aluminum Ingots During the Start-Up Phase

Werner Droste (1), Jean-Marie Drezet (2), Gerd-Ulrich Grün (1),
Wolfgang Schneider (1)

(1) VAW aluminium AG, Research and Development
P.O. Box 2468, D-53014 Bonn
Germany

(2) CALCOM SA
Parc Scientifique, PSE-EPFL, CH-1015 Lausanne
Switzerland

Abstract

Constant demands on scrap reduction and increased process performance in aluminum DC-casting require surfaces which need less scalping and start-up procedures which diminish butt sawing and decrease cracking tendencies. During the last years, there has been a big progress in thermomechanical simulation of aluminum DC-casting with focus on ingot shape and butt curl. The aluminum industry is on the way of transferring this more scientific method to a practical tool for calculating mold shapes, minimizing butt scrap and optimizing start-up procedures.

In the first section of this paper, a brief description of the model and its implementation are given. The 3-D model is based on the general purpose software Abaqus and uses a thermomechanical approach to describe the process taking into account the viscoplastic behaviour. It delivers the contraction of the rolling faces, the butt curl during the transient casting phase and the final ingot geometry. Also, strain rate and stress field at the end of casting are calculated. For evaluation and adaptation of the model to specific boundary conditions in a cast house, a production mold and bottom block system is chosen in order to compare calculations and corresponding casting trials on measured temperatures, curls and ingot geometries, which are finally presented.

Paper presented at Continuous Casting, DGM conference, Frankfurt, Germany, November 13-15, 2000.

calcom 

Let's look together at the solution

Introduction

During the last years, there have been joint activities of the European aluminum producers on developing tools for modeling aluminum DC-casting. A major part of this work was funded by the European Commission and is known as the EMPACT-program. Now these tools are going to be adapted by the aluminum companies for internal use. At VAW aluminium AG, this is carried out by integrating a 3D-thermomechanical model into their toolbox, which is based on the development work done first at Alusuisse [1] and later on within the EMPACT-program [2]. In this paper, a standard hot-top casting of 1650x600mm sized rolling ingots of an AA1050 alloy is simulated. The calculated results are compared with measured data coming from corresponding full size experiments. Special focus of the study is put on the transient start-up phase including butt curl and ingot geometry development.

Model Description

The 3D-model is realized with the general purpose software Abaqus. A detailed description can be found in [1-5], but a brief presentation of the concept will follow. Based on a finite element formulation to compute the thermomechanical development within the solidifying ingot, the model can calculate temperatures, stresses and stress induced deformation. The stress-strain dependency is handled by a viscoplastic material model within Abaqus using a rate dependent plasticity analysis. The model allows to predict the butt curl as well as the rolling faces pull in. Fluid flow influence on temperatures is taken into account by an increased heat conductivity in the molten state.

The computational domain is limited to one quarter of an ingot because of assumed symmetry. The design of the mould and the enmeshment of the ingot and the bottom block are given in Figure 1. In the present example, 96 nodes per layer are used and with a thickness of 30 mm per layer and 30 layers, a total cast length of 0.9 meters is simulated. The rather coarse enmeshment is a compromise to get a stable mathematical solution and an acceptable calculation time. Due to the bending phenomenon during butt curl, the elements in the related regions experience a large vertical displacement. Using smaller elements might cause severely distorted elements, which would stop the calculation due to numerical errors.

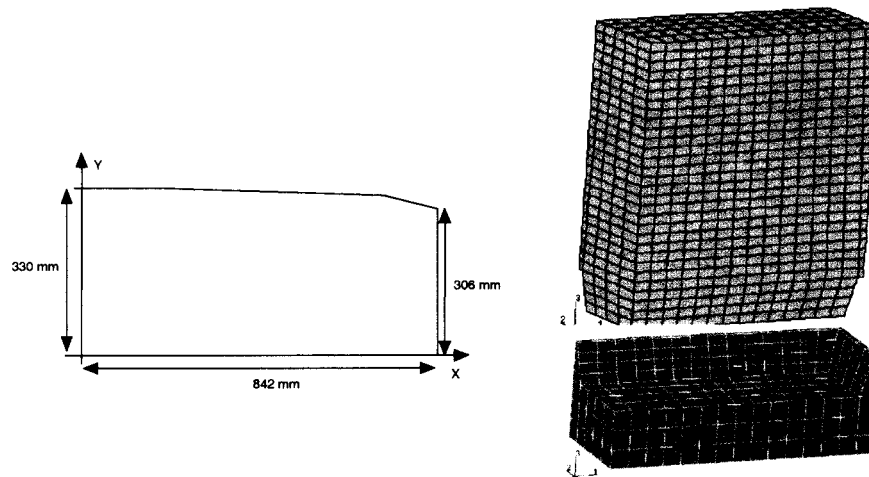


Figure 1. Mold dimensions and enmeshment of ingot and bottom block

According to the real conditions, a bowl shaped bottom block is used. Its outer rim has a height of 120 mm and follows the contour of the mould. The bottom block thickness is 180 mm, while the rim thickness decreases from 60 mm to 20 mm from bottom to top.

The material for the trials and for the simulation is an AA1050 alloy. The thermophysical and thermomechanical properties are taken mainly from the results of the EMPACT-program [2,5]. The bottom block material is an alloy of the 6000 series and it is assumed that it has constant material properties and that the bottom block will not deform at all (rigid body). The hot top, because it is considered as an insulation with adiabatic characteristics, will not influence the rolling faces pull in. Therefore, the whole region including the liquid melt is excluded in the present model.

Although, the transient start-up phase of casting is studied here, only a simplified casting recipe is applied. The liquid level in the mould is considered as constant and the filling phase starts with that melt level. Further on, a constant casting speed of 60 mm/min is chosen.

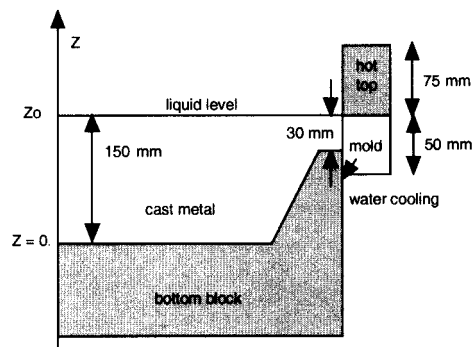


Figure 2. Initial configuration of the calculation

The initial situation is depicted in Figure 2. Five layers of metal representing a height of 150 mm are present in the bottom block at the start of the calculation. Note that the filling phase is not modeled with the present model: owing to the large convection that takes place in the liquid pool, the temperature remains rather uniform except on the outer surface of the ingot where heat transfer to the bottom block and to the mould takes place. The computation starts at the very moment when the casting table begins its descent, assuming a constant casting speed of 60 mm/min. The initial temperature field is uniform at 670°C except for the surface of the ingot which is assumed to be at 600°C.

Because Abaqus uses a Lagrangian description, metal and bottom block positions are fixed within the solution domain and the boundary conditions move upwards at casting speed on the external faces of the ingot.

The top surface of the domain is adiabatic and the temperature of each new layer is set to the temperature of the incoming metal, 670 °C, which is a reasonable choice with a temperature of about 700 °C in the launder.

According to experience, the mold length of 50 mm is subdivided into a primary cooling zone of 30 mm and a related air gap of 20 mm. All thermal boundary conditions on the external surfaces are defined as a function of the liquid metal level z and they are split in three main areas, in which different cooling mechanisms are considered:

- 1) the primary cooling (contact with the mould) with

$$\Phi = h (T - T_{\text{mould}}) \text{ for } z = (z_0 - 0.030)$$
- 2) the air gap with

$$\Phi = 0 \text{ for } (z_0 - 0.050) \leq z \leq (z_0 - 0.030)$$
- 3) secondary cooling with

$$\Phi = \text{reduct}(\text{time}) \cdot h_{\text{water}}(T) \cdot (T - T_{\text{water}}) \text{ for } z = (z_0 - 0.05)$$

where h_{water} is a surface temperature-dependent heat transfer coefficient and the $\text{reduct}(\text{time})$ -function is a coefficient to simulate the reduced amount of cooling water during start-up, which rises from 32.4 m³/h to a steady state value of 45.9 m³/h.

A more detailed description about the determination of the heat flow and the heat transfer coefficients is given in [6]. Starting with an initial temperature of 25 °C the bottom block is cooled down on its vertical sides with a constant heat transfer coefficient and a water temperature of 25 °C. On its bottom side, an air cooling is applied using a much lower heat transfer coefficient.

It is known from experience that the water intrusion into the gap between ingot and bottom block can have an influence on the butt curl. Therefore, a strategy, which simply increases the gap conductance, when water starts to intrude, is partially wrong since the intruding water represents rather a heat sink for both, the bottom block and the ingot. Models, which do not account for that, deliver butt curl results, which are too small compared to measured data. One intention of this work is to improve the agreement with measured butt curl. In order to do so, a more realistic model of the water intrusion is tested:

- 1.) remove the contact elements in the interface, where water intrudes and

- 2.) apply instead a special boundary condition on both sides of the interface, i.e. on the ingot and on the bottom block, assuming a constant heat transfer coefficient $h_{\text{intrusion}}$ and a constant water temperature.

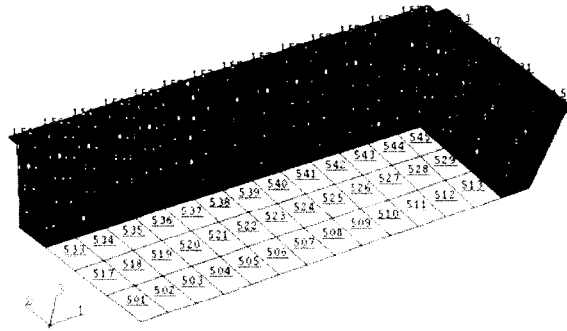


Figure 3. Top surface elements of the bottom block showing the area, where water intrusion is modeled (elements marked dark).

The water intrusion takes place at 60 s after the start of withdrawing, i.e. about 10 s after the water of the secondary cooling system starts to impinge the ingot surface (time 50 s). The dark element surfaces in Figure 3 show the area wetted by the water and where the special conditions are applied. This zone extends more or less down to the drainage holes, remaining the central area dry (white area).

Casting Experiments

The experiments were carried out using a VAW aluminium AG hot top mold system for the mentioned ingot size of 1650x600mm. Temperature in the launder and the casting temperature had the values described above. The melt distribution inside the solidifying ingot was done with a standard Combo-bag. Initially, the upper rim of the bottom block was placed about 10mm below the hot top. Water flow amount was rising during the start-up as given above, the water temperature was 23 °C. After filling the mold up to the hot top within about 4 min, the casting table was lowered first with a speed slightly slower than 62 mm/min. Entering the direct cooling zone the speed was increased slightly above the final casting speed until the final casting speed was adjusted.

During the trial casts butt curl and butt temperature development was recorded. Additionally, a detailed measurement of the butt geometry followed after the casting. The curl measurements were carried out in the middle of both small sides of the ingot using displacement transducers connected to the ingot via a 0.8mm steel rods (Figure 4).



Figure 4. Butt curl measurement equipment

The development of the curl displayed in the following figures is the mean of the measured left and right value. The grid of thermocouples was mounted inside the bottom block to measure the temperatures at a depth of about 10 mm within the ingot butt all along the x- and the y-axis and within one quarter of the ingot. In this paper only the temperatures measured along the x-axis at distances $x = 0, 150, 350, 450$ and 600mm are presented, because they will be used in the comparison with the calculations. The ingot geometry scan was done at cast lengths of 50, 150, 250, 350, 650, and 1550 mm.

Results

Figure 5 shows the comparison of the time-dependent vertical displacement of the mesh point situated at the middle of the short face of the simulated ingot (named calculated curl) with the results of a representative butt curl measurement from experiments. Additionally, the time derivative of both curves are given, which represent the related curling speed. Note that with the assumption of a rigid bottom block, the vertical displacement of the mesh corresponds to the measured butt-curl. Moreover, since the filling phase is not modeled, the time scale used for the computation has been shifted by the filling time so that the results can be compared with the measurements.

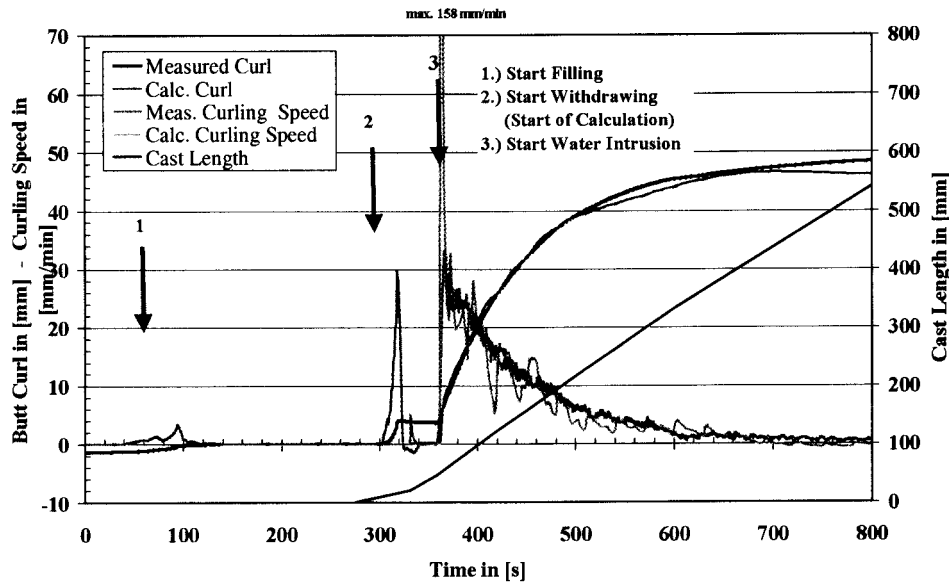


Figure 5. Measured and calculated butt curl and curling speed

Looking on the resulting butt curl development, two important events can be identified:

1. In the calculation, no curl is observed until the cooling water starts to impinge the ingot surface (time 361 sec in Figure 5). In fact, during that period, the already solidified shell is still hot and weak and therefore the ingot does not deform on the bottom block.
2. The butt curl starts at the time the secondary cooling water hits the ingot surface (time 361 sec). As soon as the water intrusion occurs, the cooling of both, the ingot and the rim of the bottom block, becomes very high. This leads to a separation of the metal from the bottom block and the butt curling starts. The measured data also seem to have some curl right at the beginning of filling though the steel rod for the curl measurement has not yet contact to the aluminum. The explanation for this behavior is the expansion of the bottom block, which starts at the beginning of filling. Due to that expansion the small gap between bottom block and mold wall is closed and the steel rod is pinched in. This causes the small offset error of about 5mm in the curl measurement (also visible at the start of withdrawing, (2) in Figure 5), which has to be subtracted from the measured final value of about 50 mm regarding the comparison with the model results.

Comparing the measured and calculated data, one can notice two significant points:

1. the calculated curl (~45mm) compares well with the measurement (~(50-5)mm)
2. the curling speed derived from the measurements and from the computation are both highest right at the beginning of curling. They also compare very well except a too pronounced computed maximum owing to the coarse mesh, which is the reason of the step like substructure in the calculated curling speed

Figure 6 shows the calculated and measured rolling face contours of the butt after it has cooled down to room temperature. The design of the mold is also shown. The butt swell is most visible at cast lengths between 50 and 350 mm. Then, the steady state contraction is measured at lengths 650 and 1550 mm. The contraction development in the butt zone is somewhat underestimated by the model by an amount of 10 mm for the ingot width, that is 5 mm on one ingot side. The use of a rather coarse mesh and/or not fully adjusted material properties or boundary conditions can explain this behavior. Also the casting speed in the calculation was constant while in the experiment a slightly higher speed was chosen.

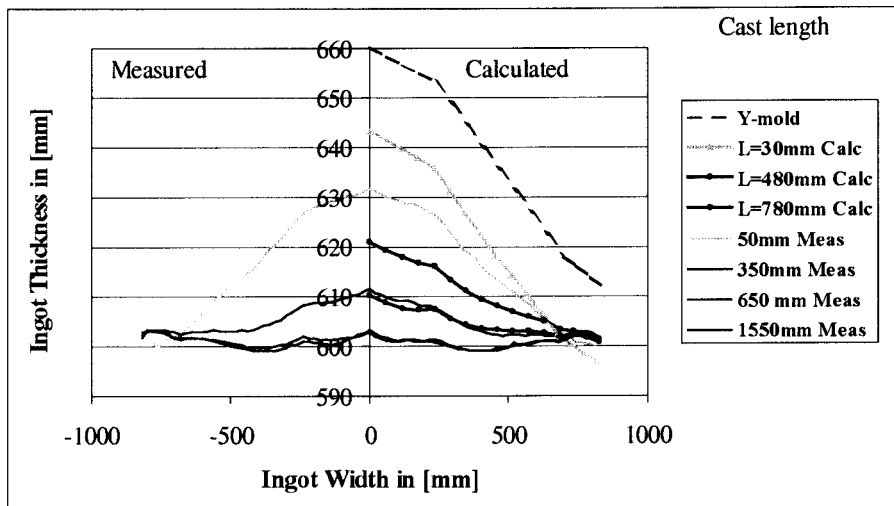


Figure 6. Measured and calculated rolling face contour at different heights of the ingot

Figure 7 shows a 3 D view of the simulated temperatures 50 seconds after the start of withdrawal. Water intrusion has not yet occurred. At this time the model shows a continuous partially solidified shell (temperatures lower than 650 °C, the coherency temperature of the alloy) along the rim of the bottom block. This shell is still too weak to deform. Note that the heat transfer to the rim is rather efficient. Beyond this time, the cooling of the ingot and the rim of the bottom block induced by the water intrusion begins to work.

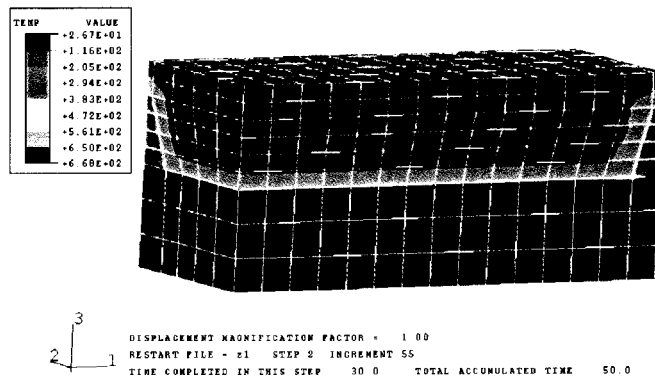


Figure 7. Temperature distribution on the deformed mesh at time = 50s.

Figure 8 shows the temperature distribution 180 seconds later (time = 50 + 6*30 s). At this time, the cooling induced by the secondary cooling is particularly efficient on the ingot. Now, the continuous shell that has built up all around the liquid pool, gets thicker where the cooling is efficient, that is near the central part of the bottom block (good thermal contact) and near the ingot surface. This shell seems to be necessary to create the stresses and strains, which cause the curling. Note that the cooling induced by the water intrusion has been very efficient for the rim but not for the ingot which remains hot.

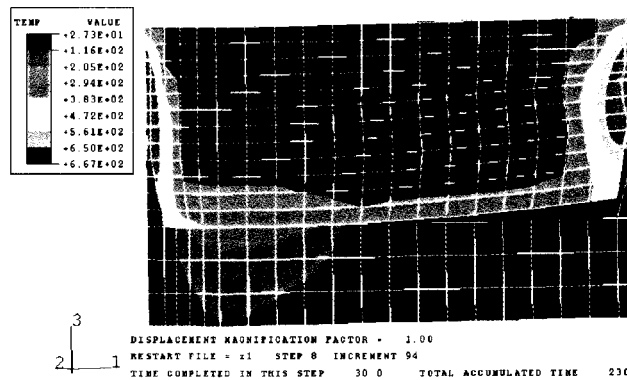


Figure 8. Temperature distribution on the deformed mesh at time = 230 s.

Figure 9 shows the temperature distribution 620 seconds after the start of withdrawal (time = 50 + 19*30s, cast length = 570 mm). Due to the development of the butt curl, the heat transfer to the bottom block is now limited to a confined area near the center, where the contact remains. Now, the increased cooling due to the water intrusion is obvious: the rigid shell shows remarkably cooler temperatures in all areas stricken by cooling water.

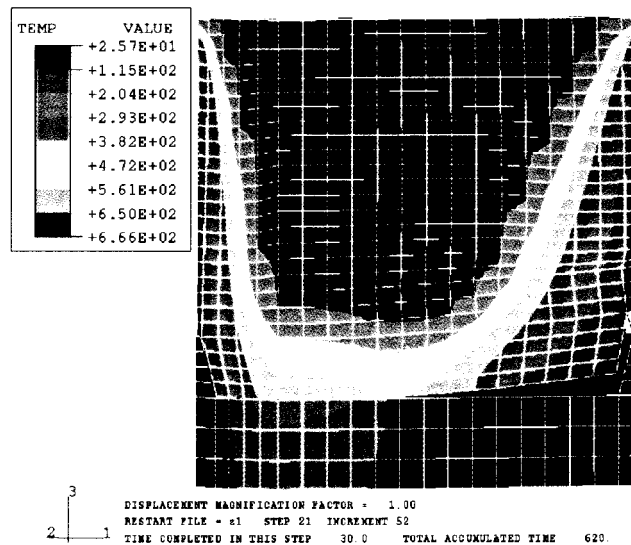


Figure 9. Temperature distribution on the deformed mesh at time = 620 s.

These calculated temperature distributions can be compared with measured temperatures at about 10 mm within the butt, shown in Figure 10.

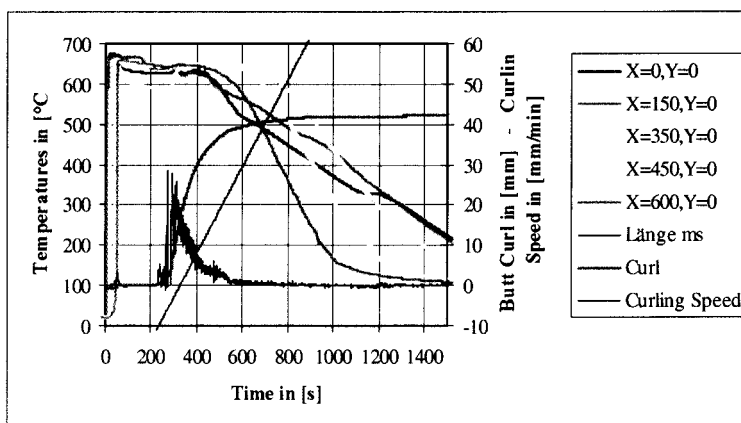


Figure 10. Measured curl and temperatures along the x-axis of the ingot 10 mm inside the butt.

The figure also includes the data of the curl measurement, which was done in parallel. The casting conditions with this experiment were exactly the same as with the curl measurement shown in Figure 6. Within the first 240s during filling, a shell has formed, and temperatures reach a minimum of about 600 °C at x = 350mm from the center. As soon as the secondary cooling hits the ingot, the butt curl starts and the temperatures rise within the butt. Only in the center at x = 0mm and 150mm the butt is still cooled by the bottom block. Even in the outer region (x=600mm), the temperatures remain at a level close to the solidus temperature for about 100s after the start of curling. This indicates, that the water intrusion needs a sufficient large gap to start a cooling effect on the bottom side of the ingot. At x = 350mm the effect of the fluid flow out of the Combo-bag is visible. This area stays close to the liquidus - solidus interval till about 700s or 500mm casting length. The general evolution of the thermal field is reproduced in an acceptable manner by the model as can be seen in Figures 7 to 9.

Conclusion

With the addition of the water intrusion effect, it is intended to better model the heat flow between ingot and bottom block. The evolution of the temperature field is now better reflected and reproduces the high cooling of ingot and rims induced by the intruding water.

Although the filling procedure has not been modeled and a rather coarse enmeshment was used, the computed butt curl compares very favorably with the measurement. As outlined, a continuous weak solidified shell around the ingot is responsible for the butt curl development.

Further work will focus on how to reduce the butt curl by notably adjusting the cooling conditions [6,7] and casting recipes and by using different bottom block geometries.

References

- [1] J.-M. Drezet, M. Rappaz, B. Carrupt, M. Plata, Metall. Trans. B, 26, 1995, 821-829
- [2] Brite-Euram Program BE-1112 EMPACT, European Modeling on Aluminum Casting Technologies, 1996-2000, Task 1.1 (thermo-mechanical tests) and Task 1.2 (sensitivity tests).
- [3] J.-M. Drezet, Ph.D. Thesis 1509, Swiss Federal Institute of Technology (1996)
- [4] J.-M. Drezet, M. Rappaz, Metall. Trans. A, 27, 1996, 3214-3225
- [5] A. Burghardt, B. Commet, J.-M. Drezet and HG Fjaer, "A numerical study of the influence of geometry and casting conditions on ingot deformation in DC casting of Al. Alloys" in MCWASP IX, TMS, Aachen, August 2000.
- [6] J.-M. Drezet, M. Rappaz, G.-U. Grün, M. Gremaud, Metall. Trans. A, 31, 2000, 1627-1634
- [7] W. Droste and W. Schneider, "Einfluß der Angießbedingungen auf die Fußgeometrie bei Aluminiumwalzbarren" in E. Lossack, Stranggießen, DGM-Informationsgesellschaft Verlag, 1991, 143-158